Acta Crystallographica Section D
Biological Crystallography
ISSN 0907-4449

Structure determination of a novel protein by sulfur SAD using chromium radiation in combination with a new crystal-mounting method

Yu Kitago, Nobuhisa Watanabe* and Isao Tanaka

Division of Biological Sciences, Graduate School of Science, Hokkaido University, Japan

Correspondence e-mail: nobuhisa@sci.hokudai.ac.jp

Received 10 December 2004
Accepted 22 April 2005

A novel and easy crystal-mounting technique was developed for the sulfur SAD method using Cr $K\alpha$ radiation (2.29 Å). Using this technique, the cryo-buffer and cryoloop around the protein crystal can be removed before data collection in order to eliminate their X-ray absorption. The superiority and reproducibility of the data sets with this mounting technique were demonstrated using tetragonal hen egg-white lysozyme crystals. The structure of a novel protein, PH1109, from *Pyrococcus horikoshii* OT3 was solved using this technique. At the wavelength of Cr $K\alpha$ radiation, the anomalous signal $\langle|\Delta F|\rangle/\langle|F|\rangle$ of PH1109 is expected to be 1.72% as this protein of 144 residues includes four methionines and two cysteines. Sulfur SAD phasing was performed using *SHELXD* and *SHELXE*. In the case of the data set obtained using this novel crystal-mounting technique, 54.9% of all residues were built with side chains automatically by *RESOLVE*. On the other hand, only 16.0% were built with side chains for the data set collected using the standard cryoloop. These results indicated that this crystal-mounting technique was superior to the standard loop-mounting method for the measurement of small anomalous differences at longer wavelength and yielded better results in sulfur-substructure solution and initial phasing. The present study demonstrates that the sulfur SAD method with a chromium source becomes enhanced and more practical for macromolecular structure determination using the new crystal-mounting technique.

1. Introduction

Use of the single-wavelength anomalous diffraction method (the SAD method, sometimes called the SAS method) is becoming increasingly common in protein crystallography. Many protein structures have been solved by the SAD method with heavy atoms such as Se, Pt, Au, Hg *etc.* using synchrotron X-rays near their absorption edge. The use of S atoms for SAD phasing is especially attractive as S atoms are present in almost all proteins (as methionine or cysteine residues) and thus neither modification such as SeMet substitution nor heavy-atom soaking is necessary for structure analysis. However, the long wavelength of the sulfur K absorption edge (5.02 Å) hampers data collection at wavelengths close to the absorption edge of sulfur and the small anomalous effect in the usual wavelength range limits the use of S atoms for SAD phasing. Thus, although sulfur SAD using Cu $K\alpha$ was

© 2005 International Union of Crystallography
Printed in Denmark – all rights reserved

Table 1
Data-collection statistics for tetragonal lysozyme.

Values in parentheses are for the last resolution shell.

	NoLoop1	NoLoop2	Loop1	Loop2	Loop3	Loop4
Crystal dimensions (mm)	0.2 × 0.2 × 0.15	0.2 × 0.2 × 0.15	0.2 × 0.2 × 0.15	0.2 × 0.2 × 0.15	0.25 × 0.25 × 0.15	0.25 × 0.25 × 0.15
Crystal-to-detector distance (mm)	80.0					
Oscillation range (°)	1.0					
Rotation range (°)	360					
Exposure time (min)	0.5	1.0	1.0	1.0	1.0	1.0
Unit-cell parameters	$a = b = 78.8$, $c = 36.9$	$a = b = 78.8$, $c = 36.9$	$a = b = 78.8$, $c = 36.9$	$a = b = 78.8$, $c = 36.9$	$a = b = 78.8$, $c = 36.9$	$a = b = 78.8$, $c = 36.9$
Space group	$P4_32_12$					
Resolution limit	50.0–2.17 (2.25–2.17)					
Reflections measured	159480	165333	163221	160396	161119	165521
Unique reflections	11692	11762	11796	11684	11775	11773
Completeness (%)	99.4 (94.2)	99.9 (99.7)	100.0 (100.0)	99.7 (100.0)	99.9 (99.7)	99.8 (98.4)
$R_{\rm sym}$ (%)	6.6 (19.2)	6.9 (17.0)	8.4 (20.6)	8.9 (23.9)	11.4 (21.7)	9.3 (18.1)
Redundancy	13.6 (7.3)	14.1 (9.8)	13.8 (8.5)	13.7 (7.6)	13.7 (8.5)	14.1 (9.9)
$I/\sigma(I)$	34.5 (9.4)	33.6 (11.6)	27.1 (9.7)	24.8 (7.9)	20.4 (9.0)	26.0 (11.7)
Mosaicity	0.486	0.394	0.566	0.526	0.403	0.420

successfully used to solve the crambin structure (Hendrickson & Teeter, 1981), there have been few reports of subsequent applications of this method. However, over the last 5 years there have been several reports of successful application of sulfur SAD phasing. These experiments were carried out using Cu $K\alpha$ radiation (1.54 Å; Bond *et al.*, 2001; de Graaff *et al.*, 2001; Yang & Pflugrath, 2001; Lemke *et al.*, 2002; Debreczeni, Bunkóczi, Girmann *et al.*, 2003; Debreczeni, Bunkóczi, Ma *et al.*, 2003) or synchrotron radiation at a wavelength of 1.54–1.77 Å (Dauter *et al.*, 1999; Liu *et al.*, 2000; Gordon *et al.*, 2001; Brown *et al.*, 2002; Li *et al.*, 2002; Micossi *et al.*, 2002; Ramagopal *et al.*, 2003; Lartigue *et al.*, 2004; Sekar *et al.*, 2004).

More recently, successful application of the sulfur SAD technique was reported using X-rays generated from a chromium target at a much longer wavelength (2.29 Å) compared with a standard Cu-target rotating-anode source (Chen *et al.*, 2004) with an X-ray apparatus optimized for protein crystallography (Yang *et al.*, 2003). As suggested by Wang (1985), the longer wavelength from a chromium target is advantageous for sulfur SAD phasing because the $\Delta f''$ value of the S atom is larger (1.14 e^-) than that obtained with Cu radiation (0.56 e^-). However, the absorption coefficients of materials also become larger at longer wavelengths. Especially in standard protein crystallography, where the crystal is mounted in a cryoloop with cryo-buffer, X-ray absorption by these materials sometimes prevents the detection of tiny anomalous signals with a high degree of accuracy. Therefore, use of the longer wavelength is still controversial.

Here, we describe a novel technique for mounting crystals that eliminates absorption effects arising from the cryo-buffer and cryoloop. This technique is especially useful for collecting data using longer wavelength X-rays for sulfur SAD phasing and can be used as easily as a conventional cryoloop. The usefulness of the new crystal-mounting technique was demonstrated using tetragonal hen egg-white lysozyme crystals and by determining the structure of an unknown protein using the anomalous signal alone from sulfur with Cr $K\alpha$ X-rays.

2. Methods

2.1. Sample preparation, diffraction data collection and processing

Hen egg-white lysozyme (Seikagaku Kogyo, Tokyo) was purchased and used without further purification. Tetragonal crystals were obtained using the hanging-drop vapour-diffusion method at 293 K. The crystallization drop consisted of 3 µl protein solution (60 mg ml^{-1}) and 3 µl reservoir solution (1.5 *M* NaCl, 100 m*M* sodium acetate buffer pH 4.2) and the reservoir volume was 1 ml. Prior to flash-cooling, the crystals were rinsed in cryoprotectant solution containing 30%(*v*/*v*) glycerol for about 30 s. In order to demonstrate the superiority and reproducibility of our mounting method, several crystals of almost identical dimensions, about 0.2 × 0.2 × 0.15 mm, were selected and used.

The novel protein PH1109 from *Pyrococcus horikoshii* OT3 used in this experiment was expressed in *Escherichia coli*, purified with HiTrap Q XL 5 ml and HiLoad 26/60 Superdex 200pg (Amersham Biosciences) and concentrated to 10 mg ml^{-1} in 10 m*M* Tris–HCl buffer pH 8.0 and 20 m*M* NaCl. PH1109 crystals were obtained using the sitting-drop vapour-diffusion method from condition No. 37 of the Cryo I screening kit from deCode Genetics (Reykjavik, Iceland) consisting of 40%(*v*/*v*) PEG 300, 0.1 *M* cacodylate buffer pH 6.5 and 0.2 *M* calcium acetate. The crystallization drop contained 1 µl protein solution and 1 µl reservoir solution and the reservoir volume was 100 µl. The crystals grew to dimensions of 0.1 × 0.1 × 0.3 mm in the sitting drop at 293 K. The crystals belonged to space group $P6_522$ and had unit-cell parameters $a = b = 70.0$, $c = 144.2$ Å. The asymmetric unit contains one protein molecule and the estimated solvent content is 58%. The overall $\langle|\Delta F|\rangle/\langle|F|\rangle$ calculated from the amino-acid sequence was 1.72% when only the S atoms (except for the first Met) were taken into account as anomalous scatterers. For data collection, crystals were mounted either using the novel device described in the next section or with a standard cryoloop. Diffraction data were collected to a

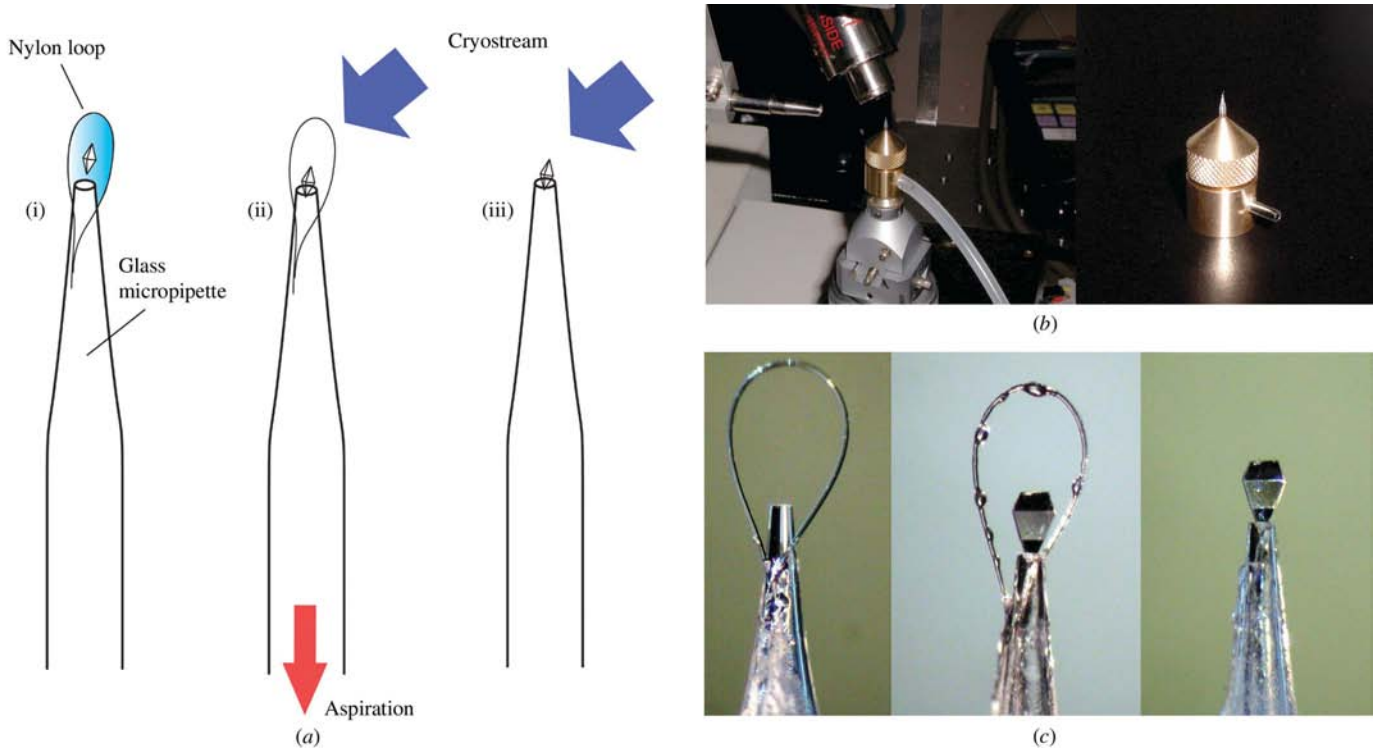

Figure 1
(*a*) A schematic illustration of the novel mounting technique. (i) Picking up a protein crystal using a nylon loop at the top of glass micropipette and mounting the tools on the goniometer head intercepting the cryostream. (ii) Aspirating the cryo-buffer through the micropipette and flushing with the cold nitrogen stream. (iii) Removing the nylon loop under cryo-conditions. (*b*) The mounting base for the novel mounting technique. This tool can hold the micropipette and aspirate the cryo-buffer through the flexible tube. (*c*) Left, the tip of the micropipette and nylon loop before picking up a protein crystal. The nylon loop was glued to the tip of the micropipette. Middle, the tip of the micropipette and a protein crystal after aspirating the cryo-buffer and freezing. Right, the tip of the micropipette and a protein crystal after removing the nylon loop. In the middle and right pictures, a thaumatin (Sigma T-7638) crystal was used as the sample.

resolution of 2.17 Å using an in-house X-ray source (Rigaku FR-E SuperBright with a Cu/Cr dual target; 40 kV, 40 mA for Cr), Osmic Confocal MaxFlux optics optimized for chromium (Cr CMF; Yang *et al.*, 2003) and a Rigaku R-AXIS VII imaging-plate detector. A 0.5 mm collimator was used to keep the whole crystal bathed in the X-ray beam. The black paper on the front of the R-AXIS VII was replaced by a carbon-filled thin polymer film in order to decrease absorption. A post-sample helium path (Yang *et al.*, 2003) and a collimator extension cap were also used to reduce absorption and scattering by air. The data-collection protocol, including highly redundant measurements, was the standard protocol for single-wavelength experiments. A total of 360 images with 1.0° oscillation were collected for lysozyme and a total of 720 images with 0.5° oscillation were collected for PH1109, with a crystal-to-detector distance of 80 mm. The exposure time for PH1109 was 1 min and that for lysozyme crystals is summarized in Table 1. For comparison, data sets were also collected with the same apparatus but using standard cryoloops of 0.4–0.5 mm diameter (20 µm nylon fibre, Hampton Research). The collected intensities were indexed, integrated, corrected for absorption, scaled and merged using *HKL*2000 (Otwinowski & Minor, 1997) with the 'scale anomalous' flag to keep Bijvoet pairs separate.

2.2. Loop-less and buffer-less mount for eliminating X-ray absorption

As described above, the X-ray absorption coefficients of materials increase at longer wavelengths. Therefore, diffraction intensities measured at low temperatures may be influenced strongly by the frozen buffer solution and the cryoloop around the crystal. To eliminate X-ray absorption by the cryo-buffer and cryoloop, we have developed a novel technique for mounting a protein crystal without them. For this purpose, a new tool was devised based on the free-mounting technique of protein crystals reported by Kiefersauer *et al.* (1996, 2000), which was originally used to improve the resolution limit of diffraction by accurately controlled humidity changes. As in their method, a glass micropipette was made using a Narishige PC-10 pipette puller (Narishige Scientific Instrument Laboratory, Japan) and the tip of the micropipette was cut and ground using a Narishige MF-900 microforge and an EG-400 micropipette grinder. Our technique is novel in that the nylon loop is glued directly onto the tip of the micropipette and fixed as if the micropipette tip is located in the loop, so the solution caught in the loop can be aspirated through the micropipette just prior to flash-freezing (Fig. 1*a*). A mounting base for airtight holding of the micro-

pipette was also made (Fig. 1*b*). Protein crystals can be picked up from the crystallization drop using the loop at the tip of the pipette and the cryo-buffer in the loop can be removed by aspiration prior to flash-freezing the crystal on the goniometer head of the diffractometer. When the cryo-buffer is removed by aspiration, the protein crystal is usually located on the tip of the micropipette, as shown in Fig. 1(*c*). The remaining cryo-loop can be torn off with a small hook or forceps with careful attention paid to the crystal.

The actual procedure for mounting a crystal was as follows. Before the crystal was picked up, the micropipette with the loop was fixed onto the mounting base and a soft tube for aspiration was connected to the base. A crystal in the cryo-buffer was picked up using the loop at the tip of the micro-pipette and the device was mounted on the goniometer head intercepting the cryostream as in the standard procedure. The cryo-buffer in the loop was removed immediately by aspiration and the crystal was flash-frozen on the tip of the micro-pipette with a stream of cold nitrogen. Finally, the glued cryoloop was removed using a micro-hook made of metal wire without disturbing the cold stream. In this way, we succeeded in freezing and holding the crystal without buffer or loop and avoiding dehydration. In most cases, these crystal-mounting procedures were not difficult and the rate of failure was almost the same as the standard cryoloop-mounting technique.

2.3. SAD phasing of PH1109 protein

To estimate the accuracy of the measurement of anomalous differences, the experimental values of $\langle|\Delta F|\rangle/\langle|F|\rangle$ and $\langle|\Delta F|\rangle/\langle\sigma(\Delta F)\rangle$ were plotted against the resolution bin. The values of $\langle|\Delta F|\rangle/\langle|F|\rangle$ were compared with the theoretical value calculated from the elemental composition estimated from the amino-acid sequence (Dauter *et al.*, 1999, 2002). The positions of anomalous scatterers were located using *SHELXD* (Sheldrick *et al.*, 2001) after analysing the substructure structure factors using *SHELXC* (Sheldrick, 2003). The initial phases were estimated by *SHELXE* (Sheldrick, 2002) with the sites and improved by density modification with a solvent content of 0.58. After *SHELXE*, the initial model was built automatically by *RESOLVE* (Terwilliger, 2000, 2003) with the build_only option. The initial model was extended and refined automatically by *Lafire* (Yao *et al.*, 2005), which implements *CNS* programs (Brünger *et al.*, 1998) for refinement. The

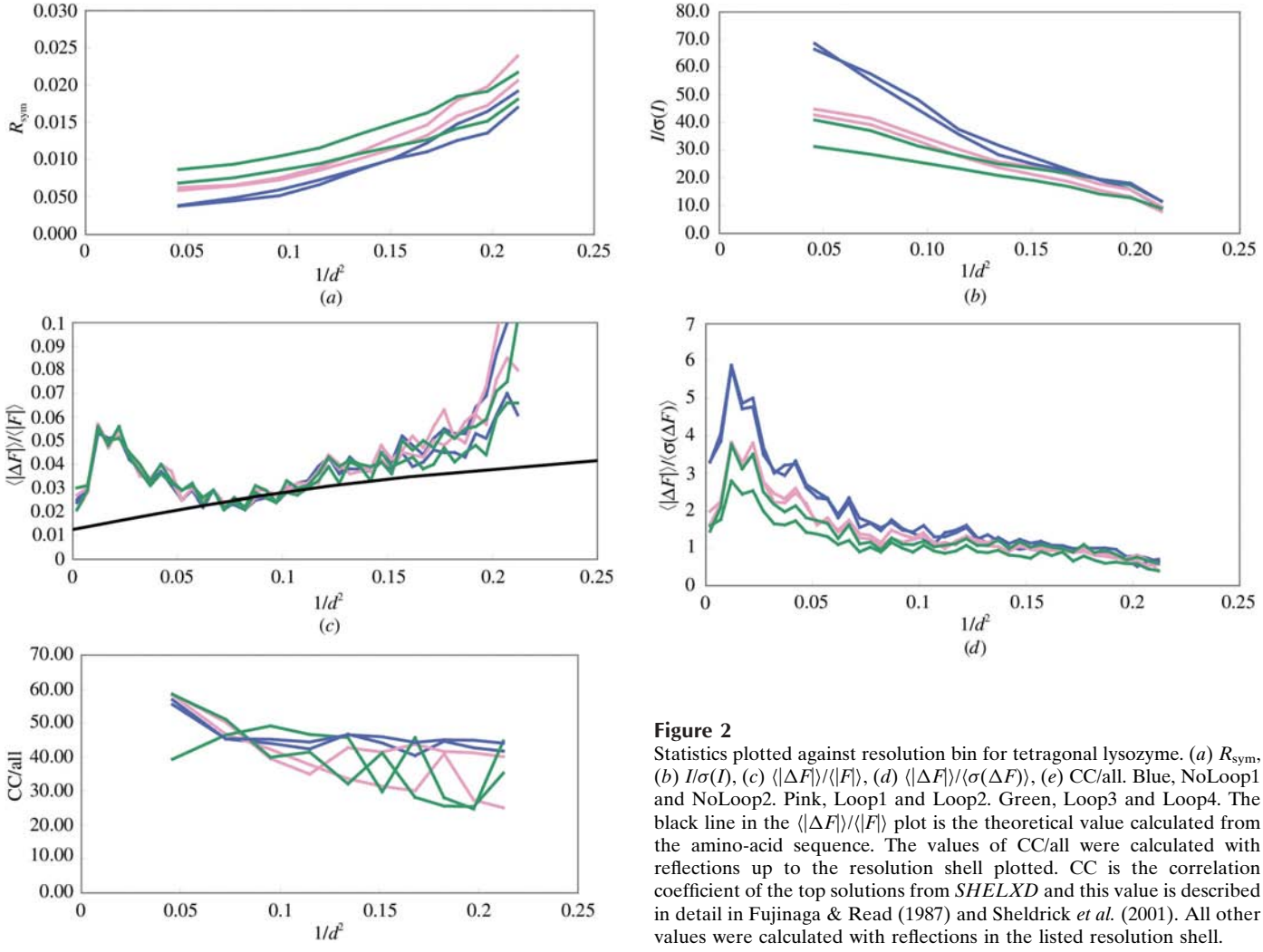

Figure 2
Statistics plotted against resolution bin for tetragonal lysozyme. (*a*) R_{sym}, (*b*) $I/\sigma(I)$, (*c*) $\langle|\Delta F|\rangle/\langle|F|\rangle$, (*d*) $\langle|\Delta F|\rangle/\langle\sigma(\Delta F)\rangle$, (*e*) CC/all. Blue, NoLoop1 and NoLoop2. Pink, Loop1 and Loop2. Green, Loop3 and Loop4. The black line in the $\langle|\Delta F|\rangle/\langle|F|\rangle$ plot is the theoretical value calculated from the amino-acid sequence. The values of CC/all were calculated with reflections up to the resolution shell plotted. CC is the correlation coefficient of the top solutions from *SHELXD* and this value is described in detail in Fujinaga & Read (1987) and Sheldrick *et al.* (2001). All other values were calculated with reflections in the listed resolution shell.

model and the improved electron-density maps were inspected using *XtalView* (McRee, 1992).

3. Results and discussion

3.1. Superiority of the mounting technique

In order to demonstrate the superiority of our mounting technique, six data sets were collected using tetragonal hen egg-white lysozyme crystals, of which two were collected with our mounting technique (named NoLoop1 and NoLoop2) and four were collected using a standard cryoloop (Loop1–Loop4). Two of the four data sets with a cryoloop (Loop3 and Loop4) were collected using about 1.5-fold larger crystals than other four crystals. The collected intensities were processed using *HKL*2000 and diffraction data statistics are shown in Table 1. The total number of measured reflections and completeness are almost the same for the nine data sets. Statistics of each data set, such as $R_{\rm sym}$, $I/\sigma(I)$, $\langle|\Delta F|\rangle/\langle|F|\rangle$ and $\langle|\Delta F|\rangle/\langle\sigma(\Delta F)\rangle$ were plotted against resolution bins and are shown in Fig. 2. The correlation coefficients (CC/all) of *SHELXD* were also calculated against resolution bins as reported by Fu *et al.* (2004). All plots show that the data with our mounting technique gave better results. The behaviour of the plots of Bijvoet ratio $\langle|\Delta F|\rangle/\langle|F|\rangle$ were not so clear, but a

Table 2
Data-collection statistics for PH1109.

Values in parentheses are for the last resolution shell.

	Using the novel technique	Using the standard loop
Crystal dimensions (mm)	0.1 × 0.1 × 0.3	0.1 × 0.1 × 0.3
Crystal-to-detector distance (mm)	80.0	
Oscillation range (°)	0.5	
Rotation range (°)	360	
Exposure time (min)	1.0	1.0
Unit-cell parameters	$a = b = 70.0$, $c = 144.2$	$a = b = 69.8$, $c = 142.9$
Space group	$P6_522$	
Resolution limit	50.0–2.17	50.0–2.17
Reflections measured	439535	410744
Unique reflections	20578	18901
Completeness (%)	98.3 (94.5)	91.5 (79.1)
$R_{\rm sym}$ (%)	5.8 (16.8)	6.7 (20.3)
Redundancy	21.4 (16.4)	31.7 (19.7)
$I/\sigma(I)$	39.6 (17.3)	33.2 (14.0)
Mosaicity	0.687	0.470

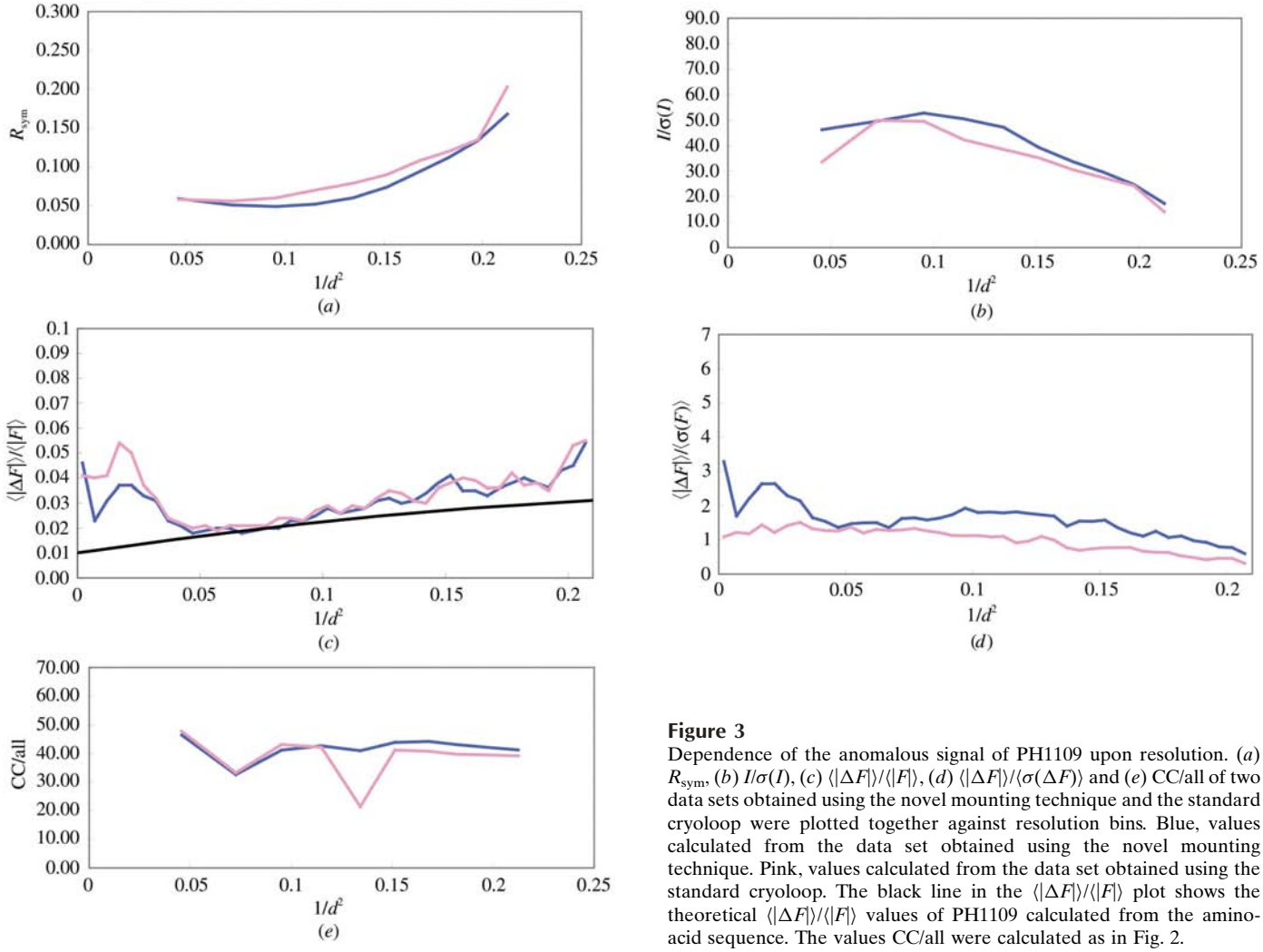

Figure 3
Dependence of the anomalous signal of PH1109 upon resolution. (*a*) $R_{\rm sym}$, (*b*) $I/\sigma(I)$, (*c*) $\langle|\Delta F|\rangle/\langle|F|\rangle$, (*d*) $\langle|\Delta F|\rangle/\langle\sigma(\Delta F)\rangle$ and (*e*) CC/all of two data sets obtained using the novel mounting technique and the standard cryoloop were plotted together against resolution bins. Blue, values calculated from the data set obtained using the novel mounting technique. Pink, values calculated from the data set obtained using the standard cryoloop. The black line in the $\langle|\Delta F|\rangle/\langle|F|\rangle$ plot shows the theoretical $\langle|\Delta F|\rangle/\langle|F|\rangle$ values of PH1109 calculated from the amino-acid sequence. The values CC/all were calculated as in Fig. 2.

tendency to overestimate the anomalous differences at higher resolution can be seen for the data sets using the cryoloop. Intriguingly, $I/\sigma(I)$ plots were not improved, even when larger size crystals were selected.

3.2. Structure solution of PH1109 protein

Data-collection statistics are summarized in Table 2. Various statistics plotted against resolution bin are shown in Fig. 3. As in the lysozyme test case, the experimental plots of the Bijvoet ratio, $\langle|\Delta F|\rangle/\langle|F|\rangle$, showed a smooth behaviour which coincided well with the theoretical curve calculated from the amino-acid sequence in the resolution range 20–2.17 Å and a difference in data quality between the two data sets was not clearly observed. However, as expected, the difference between the two data sets can be seen in the signal-to-noise ratio $I/\sigma(I)$ and $\langle|\Delta F|\rangle/\langle\sigma(\Delta F)\rangle$. The data set collected using our technique gave better statistics than the results from lysozyme crystals.

Consequently, the two mounting methods showed clear differences in sulfur-substructure determination and the phasing process. The correlation coefficient CC/all values from *SHELXD* showed a significant superiority of the novel mounting technique. The higher CC/all values indicated that the data set measured using our method had more accurate anomalous signals and was more useful for the production of the anomalous scattering substructure than the standard cryoloop-mounting procedure.

Although PH1109 contains six S atoms (four Met and two Cys, disregarding the first Met), *SHELXD* gave 11 sites as anomalous scatterers. Comparison with the final structure indicated that two of these 11 sites were P atoms of coenzyme A, which binds to the PH1109 molecule. The $\Delta f''$ value of a P atom is 0.899 e^- at a wavelength of 2.29 Å and was sufficient to be found by *SHELXD*. The other three sites seemed to be a type of ion as they were located on the surface of the protein molecule. One site may contain calcium cations, as calcium acetate was included in the crystallization conditions; this site was coordinated by seven ligands. The other two ions may be chloride anions which were included in the sample buffer. The remaining six sites were the S atoms of the PH1109 molecule. After SAD phasing and density modification by *SHELXE*, the electron-density map obtained was of quite good quality as shown in Fig. 4(*a*). Most of the secondary structure and some distinctive side chains, such as Tyr or Trp, were clearly identified. As a result of auto-building by *RESOLVE*, 109 of the 144 residues were traced and of these 79 residues were identified with their side chains (Fig. 5*a*). The final model after automatic model extension and refinement by *Lafire* contained 142 of 144 residues (Fig. 5*b*). The C-terminal two residues are disordered and were not found in the electron-density map. However, the bound coenzyme A was found in the electron-density map.

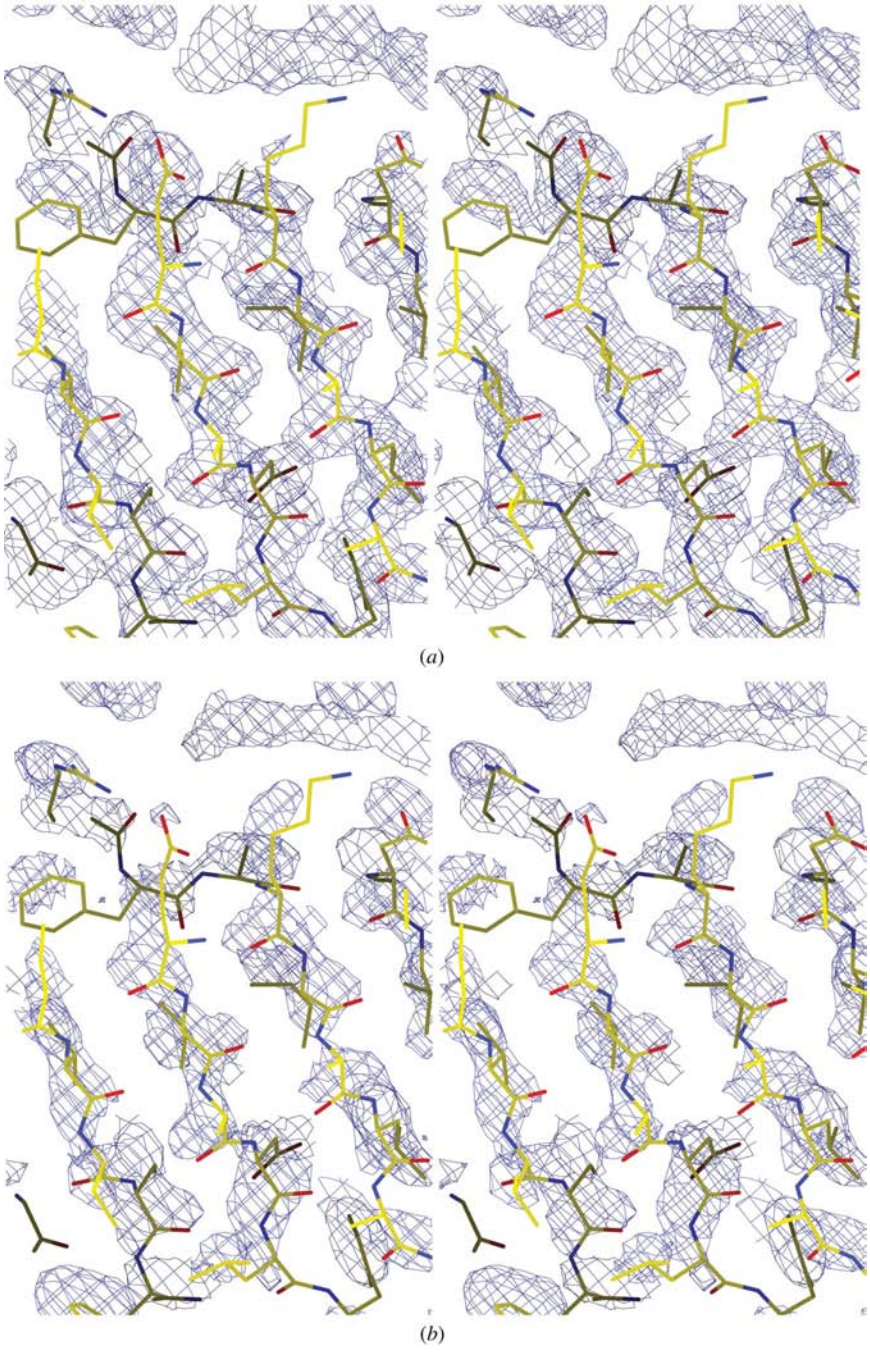

Figure 4
Stereoview of the initial electron-density map of PH1109 at the 2.0σ level calculated using the phases estimated by *SHELXE* at a resolution of 2.17 Å. (*a*) Using our mounting method. (*b*) Using standard cryoloop method. The model in the figure is the refined model.

The differences in the phasing results between the data sets using the novel mounting technique and those using the standard cryoloop are summarized in Table 3. The large differences in the number of residues built by *RESOLVE* clearly demonstrated that our crystal-mounting method is superior to the conventional method in practical use. Almost all the models were traced automatically using the data measured with our crystal-mounting technique. On the other hand, the data obtained using the standard cryoloop gave many short fragments, as shown in Fig. 5(*c*). Compared with the electron-density map calculated using the data sets of our mounting method, the map of the data set using the standard cryoloop is poorer, as shown in Fig. 3.

As shown in Table 2, the completeness of the data set collected using the standard cryoloop was a little poorer than the data set with our mounting method because the *c** axis was accidentally aligned with the spindle of the diffractometer. In order to remove this bias, only the same reflections as the standard cryoloop data set were extracted from the data set with our mounting method and the same analysis was performed. The results and statistics are also summarized in Table 3. Although the result of *RESOLVE* auto-tracing was a little poorer than that of the original data set, the superiority of our crystal-mounting method was retained, as shown in Fig. 5 and Table 3.

The result of the present study suggested that absorption correction by *SCALEPACK* could not correct the measured intensity adequately when the standard cryoloop was used with longer wavelength X-rays because the levels of X-ray absorption of the cryo-buffer and the nylon loop were much

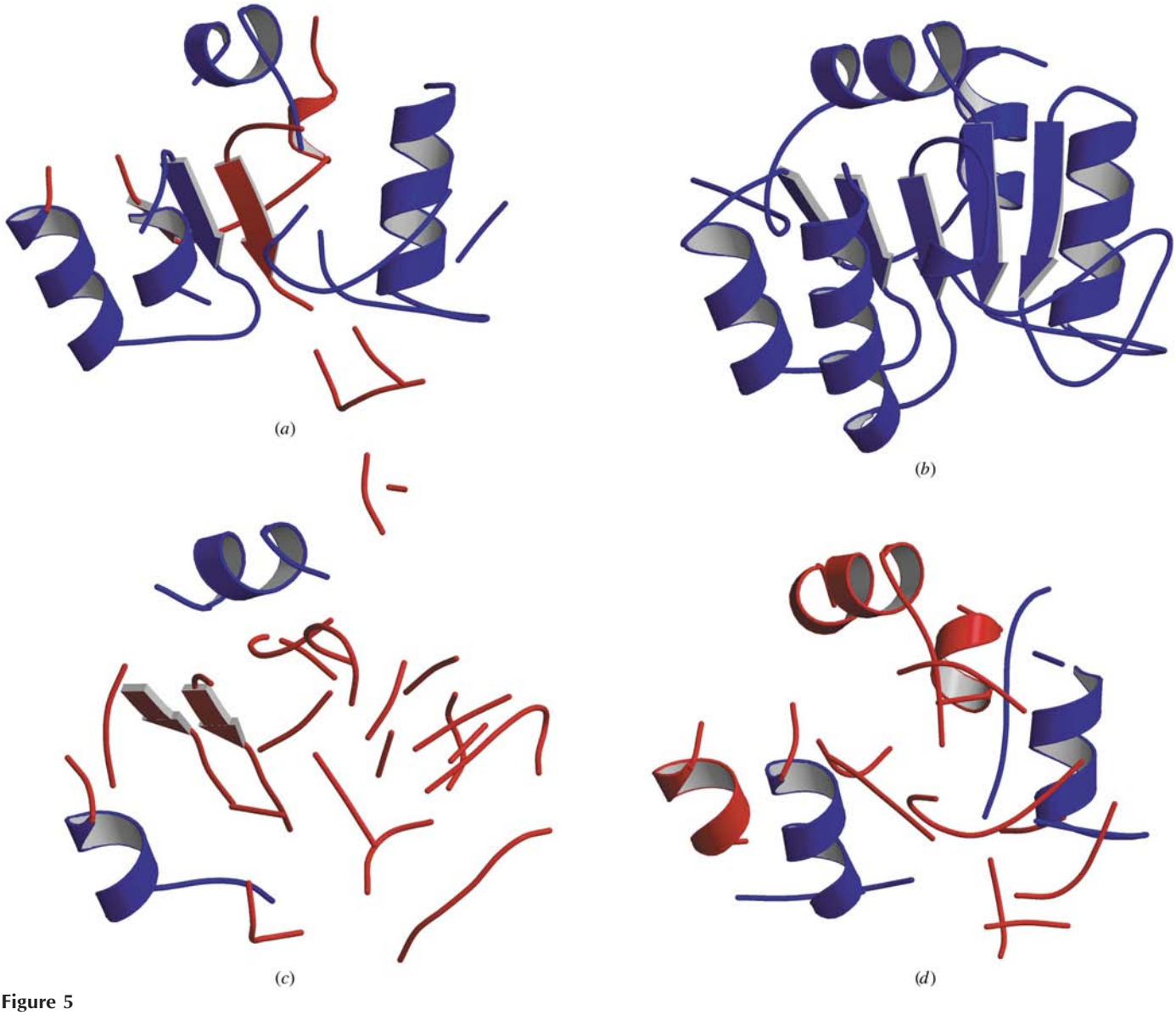

Figure 5
(*a*) Overview of the initial model of PH1109 built by *RESOLVE* using the data set from our crystal-mounting method. The model identified without side chains is shown in red and that with side chains is shown in blue. (*b*) The final model constructed by *Lafire*. (*c*) The initial model produced from the data set obtained using the standard cryoloop built by *RESOLVE*. The colours are the same as in (*a*). (*d*) The initial model produced using an extracted data set that has only the same reflections as the data set with the standard loop.

Table 3
The differences of several parameters between the data sets of PH1109.

After density modification by *SHELXE*, the map CCs were compared between the data sets. The reference maps for map CC were calculated using the final models for each data set without water molecules. (R and R_{free} were 27.0 and 23.0% for our mounting method and 27.1 and 22.1% for the standard cryoloop, respectively.) The results for extracted data are also shown.

	Using the novel technique		
	Original	Extracted	Using the standard cryoloop
No. of reflections used in *SHELX*			
Total No. of reflections	20555	18954	18901
No. of unique reflections	11440	10459	10459
SHELXD			
CC/all	41.21	41.49	38.72
CC/weak	21.95	21.52	18.64
PATFOM	10.55	10.42	8.60
SHELXE			
CC between E_{obs} and E_{calc}	38.19	38.99	35.19
No. of residues built by *RESOLVE*			
With side chains	79	42	23
Without side chains	33	69	86
Map CC with refined map			
Map after phasing	0.515	0.497	0.363
Map after density modification	0.830	0.808	0.593

larger and their shapes were not related to that of the protein crystal inside them. The scale factor estimated by *SCALEPACK* for the data obtained using the standard cryoloop and our device are plotted together in Fig. 6. The data set obtained using the standard cryoloop showed a large amplitude of modulation owing to the frozen cryo-buffer and the cryoloop. On the other hand, the data set obtained using our technique showed smooth behaviour. These results clearly indicated that the effects of absorption by the cryo-buffer and the cryoloop decreased markedly using our mounting technique. Using our mounting technique, the absorption correction function could be estimated for the protein crystal itself and applied appropriately to the measured intensity data.

4. Conclusions

The results of the present study indicated that our crystal-mounting technique can effectively increase the accuracy of measured anomalous differences. The results obtained using our technique showed clear superiority to those obtained with the standard cryoloop in structure determination by the sulfur SAD method. We succeeded in determining the structure of PH1109 protein by the sulfur SAD method using an in-house chromium X-ray source and the novel crystal-mounting technique. We have also solved three other novel protein structures, two of which have molecular weights of 68 and 84 kDa, using our mounting method (manuscripts in preparation). The estimated Bijvoet ratios, $\langle|\Delta F|\rangle/\langle|F|\rangle$, of each protein were 1.04 and 1.68%, respectively. We think that the sulfur SAD method using Cr $K\alpha$ radiation will become a practical means for determination of the structures of native proteins with our novel crystal-mounting method.

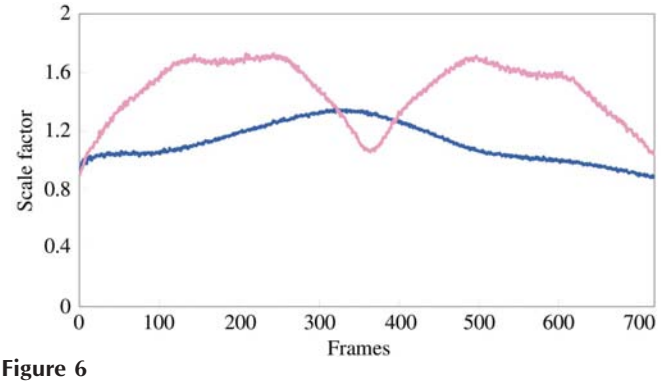

Figure 6
Scale-factor plot of PH1109 against frames. Blue, the data set obtained using the novel mounting technique. Pink, the data set obtained using the standard cryoloop.

We thank Dr Min Yao for allowing us to use PH1109 samples for this study. This work was supported by a research grant from the National Project on Protein Structural and Functional Analysis from the Ministry of Education, Culture, Sports, Science and Technology of Japan.

References

Bond, C. S., Shaw, M. P., Alphey, S. & Hunter, W. N. (2001). *Acta Cryst.* D**57**, 755–758.
Brown, J., Esnouf, R. M., Jones, M. A., Linnell, J., Harlos, K., Hassan, A. B. & Jones, E. Y. (2002). *EMBO J.* **21**, 1054–1062.
Brünger, A. T., Adams, P. D., Clore, G. M., DeLano, W. L., Gros, P., Grosse-Kunstleve, R. W., Jiang, J.-S., Kuszewski, J., Nilges, M., Pannu, N. S., Read, R. J., Rice, L. M., Simonson, T. & Warren, G. L. (1998). *Acta Cryst.* D**54**, 905–921.
Chen, L., Chen, L., Zhou, X. E., Wang, Y., Kahsai, M. A., Clark, A. T., Edmondson, S. P., Liu, Z., Rose, J. P., Wang, B.-C., Meehan, E. J. & Shriver, J. W. (2004). *J. Mol. Biol.* **341**, 73–91.
Dauter, Z., Dauter, M., de La Fortelle, E., Bricogne, G. & Sheldrick, G. M. (1999). *J. Mol. Biol.* **289**, 83–92.
Dauter, Z., Dauter, M. & Dodson, E. (2002). *Acta Cryst.* D**58**, 494–506.
Debreczeni, J. É., Bunkóczi, G., Girmann, B. & Sheldrick, G. M. (2003). *Acta Cryst.* D**59**, 393–395.
Debreczeni, J. É., Bunkóczi, G., Ma, Q., Blaser, H. & Sheldrick, G. M. (2003). *Acta Cryst.* D**59**, 688–696.
Graaff, R. A. G. de, Hilge, M., van der Plas, F. L. & Abrahams, J. P. (2001). *Acta Cryst.* D**57**, 1857–1862.
Fu, Z.-Q., Rose, J. P. & Wang, B.-C. (2004). *Acta Cryst.* D**60**, 499–506.
Fujinaga, M. & Read, R. J. (1987). *J. Appl. Cryst.* **20**, 517–521.
Gordon, E. J., Leonard, G. A., McSweeney, S. & Zagalsky, P. F. (2001). *Acta Cryst.* D**57**, 1230–1237.
Hendrickson, W. A. & Teeter, M. M. (1981). *Nature (London)*, **290**, 107–113.
Kiefersauer, R., Stetefeld, J., Gomis-Rüth, F. X., Romão, M. J., Lottspeich, F. & Huber, R. (1996). *J. Appl. Cryst.* **29**, 311–317.
Kiefersauer, R., Than, M. E., Dobbek, H., Gremer, L., Melero, M., Strobl, S., Dias, J. M., Soulimane, T. & Huber, R. (2000). *J. Appl. Cryst.* **33**, 1223–1230.
Lartigue, A., Gruez, A., Briand, L., Blon, F., Bézirard, V., Walsh, M., Pernollet, J.-C., Tegoni, M. & Cambillau, C. (2004). *J. Biol. Chem.* **279**, 4459–4464.
Lemke, C. T., Smith, G. D. & Howell, P. L. (2002). *Acta Cryst.* D**58**, 2096–2101.
Li, S., Finley, J., Liu, Z.-J., Qiu, S.-H., Chen, H., Luan, C.-H., Carson, M., Tsao, J., Johnson, D., Lin, G., Zhao, J., Thomas, W., Nagy, L. A., Sha, B., DeLucas, L. J., Wang, B.-C. & Luo, M. (2002). *J. Biol. Chem.* **277**, 48596–48601.

Liu, Z.-J., Vysotski, E. S., Chen, C.-J., Rose, J. P., Lee, J. & Wang, B.-C. (2000). *Protein Sci.* **9**, 2085–2093.
McRee, D. E. (1992). *J. Mol. Graph.* **10**, 44–46.
Micossi, E., Hunter, W. N. & Leonard, A. G. (2002). *Acta Cryst.* D**58**, 21–28.
Otwinowski, Z. & Minor, W. (1997). *Methods Enzymol.* **276**, 307–326.
Ramagopal, U. A., Dauter, M. & Dauter, Z. (2003). *Acta Cryst.* D**59**, 1020–1027.
Sekar, K., Rajakannan, V., Velmurugan, D., Tamane, T., Thirumurugan, R., Dauter, M. & Dauter, Z. (2004). *Acta Cryst.* D**60**, 1586–1590.
Sheldrick, G. M. (2002). *Z. Kristallogr.* **217**, 644–650.
Sheldrick, G. M. (2003). *SHELXC.* Göttingen University, Germany.
Sheldrick, G. M., Hauptman, H. A., Weeks, C. M., Miller, M. & Usón, I. (2001). *International Tables for Crystallography*, Vol. *F*, edited by E. Arnold & M. G. Rossmann, pp. 333–351. Dordrecht: Kluwer Academic Publishers.
Terwilliger, T. C. (2000). *Acta Cryst.* D**56**, 965–972.
Terwilliger, T. C. (2003). *Acta Cryst.* D**59**, 38–44.
Wang, B.-C. (1985). *Methods Enzymol.* **115,** 90–112.
Yang, C. & Pflugrath, J. W. (2001). *Acta Cryst.* D**57**, 1480–1490.
Yang, C., Pflugrath, J. W., Courville, D. A., Stence, C. N. & Ferrara, J. D. (2003). *Acta Cryst.* D**59**, 1943–1957.
Yao, M., Zhou, Y. & Tanaka, I. (2005). Manuscript in preparation.